CONTACT MODELLING OF COMPOSITE STRUCTURES USING ADVANCED STRUCTURAL THEORIES

Italian Association of Aeronautics and Astronautics
XXV International Congress
9-12 September 2019 | Rome, Italy

CONTACT MODELLING OF COMPOSITE STRUCTURES USING ADVANCED STRUCTURAL THEORIES

M. H. Nagaraj[1], I. Kaleel[1], E. Carrera[1*] and M. Petrolo[1]

[1]MUL[2] Group, Department of Mechanical and Aerospace Engineering, Politecnico di Torino, Corso Duca degli Abruzzi 24, Torino, Italy

E-mail: manish.nagaraj@polito.it, ibrahim.kaleel@polito.it, erasmo.carrera@polito.it, marco.petrolo@polito.it

ABSTRACT

The current work deals with the development of contact modelling capabilities in the framework of the Carrera Unified Formulation (CUF), which is a generalised framework for the development of advanced structural theories. The current modelling approach uses 1D elements with Lagrange polynomials being used to enhance the cross-section kinematic field, leading to a layer-wise model and involving purely displacement degrees of freedom. Such a modelling approach results in 3D-like accuracy of the solution, at a significantly reduced computational effort compared to standard 3D – FEA. The current work considers normal, frictionless contact with a node-to-node discretisation, and the penalty approach is used to enforce the contact constraints. The resulting nonlinear analysis is implicitly solved using the Newton-Raphson method. The use of layer-wise modelling in CUF results in a high-fidelity solution which is capable of accurately evaluating the interlaminar stress fields, as well as accounting for transverse stretching. The development is extended to the case of dynamic contact, which uses a combination of node-to-node discretisation and Lagrange Multiplier constraints to model contact. Initial assessments consider elastic impact between two bodies and demonstrate the capability of CUF models in accurately modelling contact/impact.

Keywords: High-order modelling, CUF, contact modelling, impact

1 INTRODUCTION

Mechanical systems frequently involve physical contact among their various components, for instance the meshing of gear teeth. Contact can also occur in processes such as sheet metal forming, and in material characterisation tests such as indentation and three-point bending. Contact mechanics thus plays an important role in structural analysis, and by extension, in computational mechanics, where it still remains a challenging issue [1].

The earliest analytical formulation for contact was developed by Hertz, who applied the theory of elasticity to model contact between two elastic spheres [2]. Analytical solutions to contact problems are limited [3] and hence, over the past few decades, research has been focused on numerical approaches to contact modelling. Contact modelling techniques can be classified based on the discretisation used for the contact surface. The earliest solutions to contact analysis were based on node-to-node algorithms, where the contact constraints were enforced at a nodal level [4]. Such methods however have limited applications due to requirements of mesh compatibility at the contacting surface. The issue of compatibility requirements was alleviated by the development of node-to-surface contact algorithms, where a *slave* node is prevented from penetrating a *master* surface [5-8]. The limitation of such methods is that they do not place

constraints on *master* nodes penetrating the *slave* surface. This can be overcome by the use of two-pass methods i.e. running the node-to-surface algorithm twice and switching the *master* and *slave* definitions, but often leads to an over-constrained system. Recent efforts have been focused on the development of surface-to-surface contact algorithms, where the contact constraint is enforced in a weak or integral form over the contact surfaces [9-12].

The present work deals with the development of contact modelling capabilities in the Carrera Unified Formulation (CUF) [13]. CUF is a generalised framework to develop advanced 1D and 2D structural theories. Expansion functions are used to enhance the kinematic field across the cross-section and through the thickness for 1D and 2D models, respectively, which results in 3D-like quality of results without incurring a corresponding computational expense [14]. The current work deals with cases involving normal, frictionless contact, and a node-to-node contact algorithm has been implemented with the penalty method of contact enforcement, to solve the contact problem.

The paper is structured in the following manner. The CUF framework and an overview of contact mechanics and its implementation in CUF have been presented in Section 2. The numerical assessments and results are discussed in Section 3, followed by the conclusions in Section 4.

2 METHODOLOGY

2.1 Carrera Unified Formulation

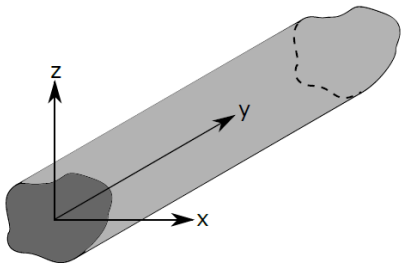

Figure 1: Beam element aligned in the CUF coordinate system

Consider a 1D element, shown in Figure 1, which is aligned in the CUF coordinate system. The generalized displacement field can be written as

$$u(x, y, z) = F_\tau(x, z)u_\tau(y), \tau = 1,2, \dots, M \tag{1}$$

where $F_\tau(x, z)$ is an expansion function described across the beam cross-section, u_τ is the generalized displacement vector, and M is the number of terms in $F_\tau(x, z)$. The expansion function and the number of terms M can be arbitrarily chosen and is a user input. The present work exploits the Component-Wise (CW) approach, where 2D Lagrange polynomials are used to enrich the cross-sectional kinematic field of 1D finite element. Such a formulation results in a layer-wise modelling of the structure and consists of only displacement degrees of freedom. The displacement field is obtained in the following manner

$$u_x = \sum_{i=1}^{n} F_i(x, z)u_{x\mathrm{i}}(y) \tag{2}$$

where *x* denotes the displacement component of a node, and *i* is the node number. More information on the use of Lagrange polynomials as expansion functions can be found in [15].

Finite Element Formulation

The stress and strain fields are given by

$$\boldsymbol{\sigma} = \{\sigma_{xx}\ \sigma_{yy}\ \sigma_{zz}\ \sigma_{xy}\ \sigma_{xz}\ \sigma_{yz}\} \tag{3}$$

$$\boldsymbol{\varepsilon} = \{\varepsilon_{xx}\ \varepsilon_{yy}\ \varepsilon_{zz}\ \varepsilon_{xy}\ \varepsilon_{xz}\ \varepsilon_{yz}\} \tag{4}$$

The linear strain-displacement relation is given by

$$\boldsymbol{\varepsilon} = \mathbf{D}\mathbf{u} \tag{5}$$

where **D** is the linear differentiation operator. The constitutive relation is given by

$$\boldsymbol{\sigma} = \boldsymbol{C}\boldsymbol{\varepsilon} \tag{6}$$

where **C** is the material stiffness matrix. Using 1D elements along the beam length, with shape functions N_i (y), the 3D displacement field is written as

$$\mathbf{u}(x, y, z) = F_\tau(x, z)N_i(y)\mathbf{u}_{\tau i} \tag{7}$$

From the principle of virtual displacements,

$$\delta W_{int} = \delta W_{ext} \tag{8}$$

where δW_{int} is the virtual variation of the internal work and δW_{ext} is that of the external work due to the applied forces. The virtual variation of the former is given by

$$\delta W_{int} = \int_l \int_\Omega \delta\boldsymbol{\varepsilon}^T\boldsymbol{\sigma}\, d\Omega dl \tag{9}$$

where *l* represents the beam length and *Ω* is the beam cross-section. The fundamental nucleus, which is a 3x3 matrix, can now be formulated based on Equations 5-8 and is given below

$$\mathbf{k}_{ij\tau s} = \int_l \int_\Omega \mathbf{D}^T\big(N_i(y)F_\tau(x, z)\big)\boldsymbol{C}\mathbf{D}\big(N_i(y)F_\tau(x, z)\big)d\Omega dl \tag{10}$$

Looping through the four indices {i, j, τ, s} results in the element stiffness matrix, which is then assembled to obtain the global stiffness matrix of the structure. A comprehensive overview of the fundamental nucleus and its role in CUF can be found in [13].

2.2 Contact modelling in CUF

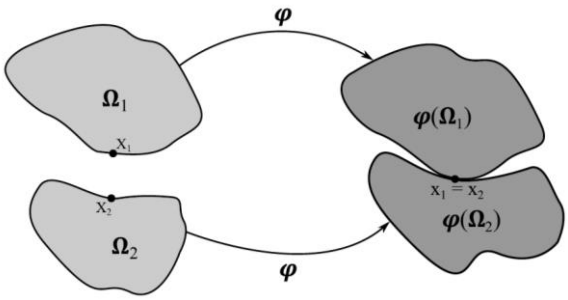

Figure 2: Two discrete bodies coming into contact under an applied deformation

Consider two discrete bodies, Ω_1 and Ω_2, as shown in Figure 2. The points $\mathbf{X}_1$ and $\mathbf{X}_2$ on the boundaries of the respective bodies come into contact due to an applied deformation $\boldsymbol{\varphi}$. The current position of the points is given by

$$\mathbf{x_i} = \mathbf{X_i} + \mathbf{u_i},\ \mathrm{i} = 1,2 \tag{11}$$

where u_i is the displacement of the point $\mathbf{X}_i$. At the moment of contact, the two distinct points $\mathbf{X}_1$ and $\mathbf{X}_2$ become coincident in the deformed configuration i.e. $\mathbf{x}_1 = \mathbf{x}_2$. Such a case of contact can be modelled using geometric constraints such as the non-penetration condition. This requires a gap function, defined below as

$$g_N = (\mathbf{u_2} - \mathbf{u_1}) \cdot \mathbf{n_1} + g_{\mathrm{init}} \geq 0 \tag{12}$$

where n_1 is the normal to the body Ω_1, and g_{init} is the initial gap between the bodies, given as

$$g_{\mathrm{init}} = (\mathbf{X_2} - \mathbf{X_1}) \cdot \mathbf{n_1} \tag{13}$$

The variational form of the contact BVP is given by

$$\delta L_{int} \geq \delta L_{ext} + \delta L_C \tag{14}$$

where δL_C is the variational work due to contact. Considering the penalty approach for the enforcement of the contact constraint, the work due to contact be written as

$$L_C = \frac{1}{2}\int_{\partial\Omega_C} \epsilon_N g_N^2 dA \tag{15}$$

with its virtual variation given by

$$\delta L_C = \int_{\partial\Omega_C} \epsilon_N g_N \delta g_N dA \tag{16}$$

where ϵ_N is the penalty parameter. In the case of node-to-node contact, the constraints are enforced at a nodal level. Using the penalty approach, the global equilibrium equation becomes

$$[\boldsymbol{K} + \boldsymbol{K^p}]\boldsymbol{U} = \overline{\boldsymbol{F}} \tag{17}$$

where $\mathbf{K}^p$ is the global contact penalty stiffness matrix, and is obtained by assembling the penalty stiffness $\mathbf{k}_i$ for a given node pair i, defined below as

$$\boldsymbol{k}_i^p = \epsilon_N \boldsymbol{n}_i^T \boldsymbol{n}_i \tag{18}$$

where $\mathbf{n}_i$ is the normal between the node pair *i*. Similarly, the contact force between the node pair *i* is given by

$$\boldsymbol{F}_i^c = \epsilon_N g_N \boldsymbol{n} \tag{19}$$

The righthand side of Equation 17 can now be written as

$$\overline{\boldsymbol{F}} = \boldsymbol{F}^{\boldsymbol{C}} + \boldsymbol{F}_{ext} \tag{20}$$

3 NUMERICAL RESULTS

3.1 3-point bending of a laminated beam

The current numerical assessment considers a laminated composite beam subjected to a 3-point bending test. The test setup has been schematically shown in Figure 3. The laminated beam is composed of 8 layers, with a stacking sequence of $[0/90]_{2s}$. The material system used is IM7-8552, whose properties have been listed in Table 1. A prescribed displacement u_z = -1.0 mm has been applied on the central roller.

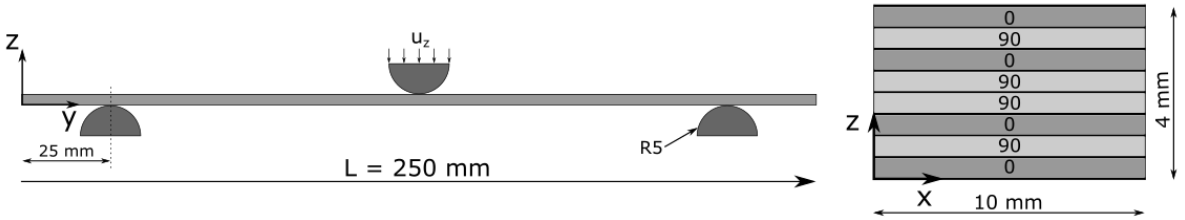

Figure 3: Schematic representation of the laminated beam under 3-pt bending

E_{11} [Gpa]	E_{22} [Gpa]	E_{33} [Gpa]	ν_{12}	ν_{13}	ν_{23}	G_{12} [Gpa]	G_{13} [Gpa]	G_{23} [Gpa]
165.0	9.0	9.0	0.34	0.34	0.5	5.6	5.6	2.8

Table 1: Material properties of the IM7/8552 system

The above structure has been analysed using the CUF-LW modelling approach, and reference numerical solutions have been developed using ABAQUS-3D. Modelling information related to the two approaches has been reported in Table 2. The results have been reported in the following: Figure 4(a) shows the vertical deflection u_z along the line joining [5.0, 0.0,4.0] and [5.0, 250.0, 4.0], i.e. the longitudinal axis of the top surface of the beam. The axial stress σ_{yy} along the same line has been plotted in Figure 4(b). The axial strain ϵ_{yy} and axial stress σ_{yy}, through the thickness of the laminate at the midspan, have been plotted in Figures 5(a) and 5(b), respectively. The axial strain ϵ_{yy} and axial stress σ_{yy} distribution through the cross-section, at the beam midspan, have been shown in Figure 6 and Figure 7, respectively.

Model	Beam Discretisation	Total DOF	Analysis Time [s]
ABAQUS – 3D	27,200 C3D8R, 3 elements per layer	399,366	1313
CUF - LW	20 B4 – 32 L9	34,236	326

Table 2: Mesh information for the various numerical models of the laminated beam

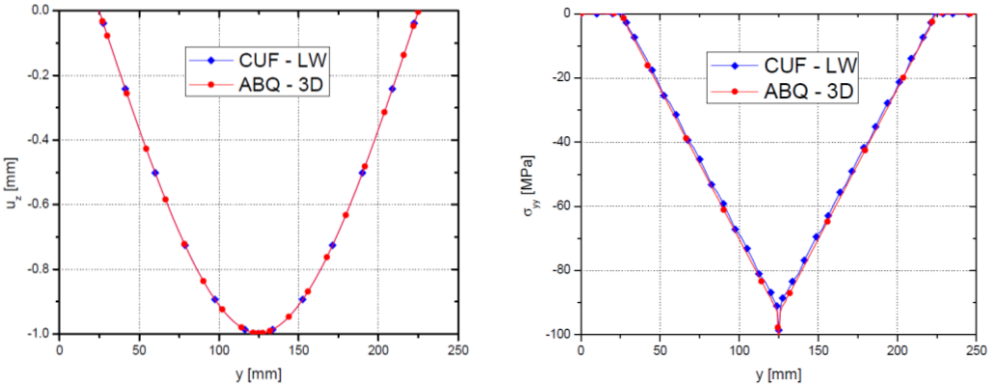

Figure 4: (a) Vertical displacement u_z, and (b) axial stress σ_{yy} along the axis of the beam

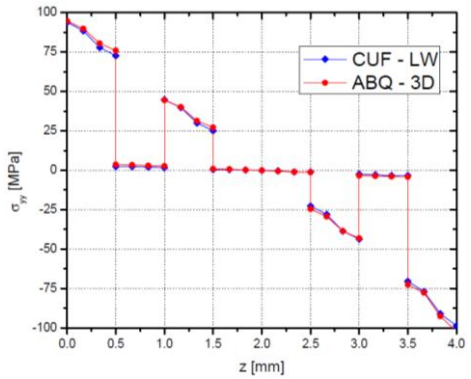

Figure 5: Axial stress σ_{yy} through the thickness of the beam at its midspan

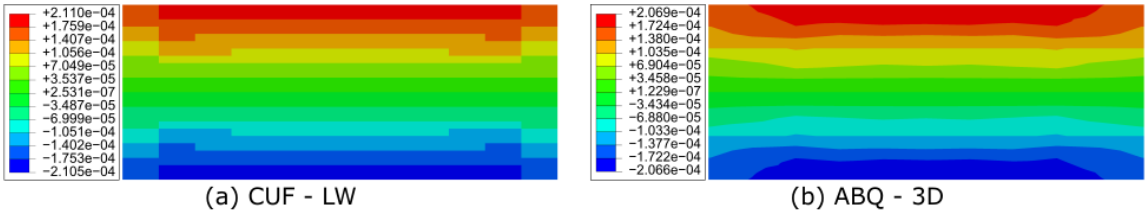

Figure 6: Distribution of the transverse strain ε_{zz} through the cross-section at [y = 150]

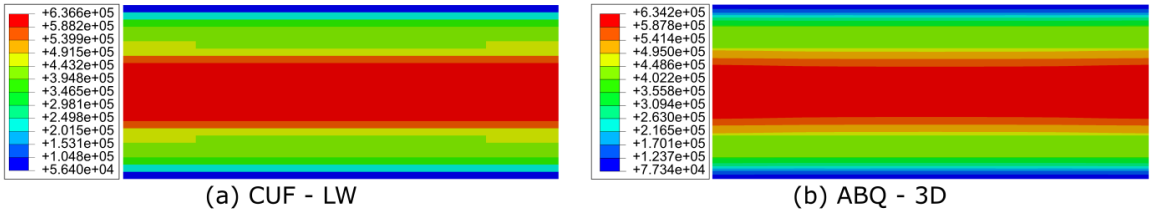

Figure 7: Distribution of the transverse shear stress σ_{yz} through the cross-section at [y = 150]

The following comments are made

1. The current approach is capable of modelling an arbitrary number of structural entities, and accounts for contact interactions among them.
2. The layer-wise modelling approach results in accurate stress fields through the thickness and can account for transverse stretching.
3. The CUF – LW model requires over 11x fewer degrees of freedom and about 4x less computational time than the 3D-FE model, for comparable quality of results.

3.2 Impact between two elastic rods

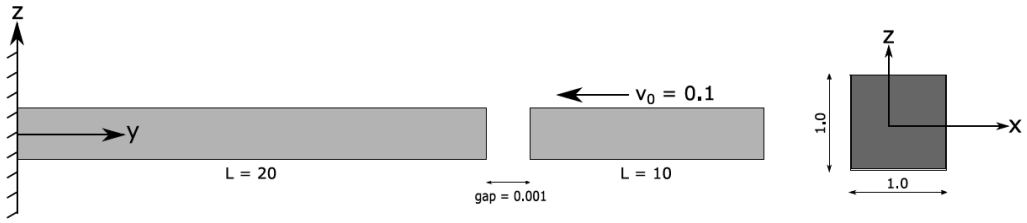

Figure 8: Schematic representation of impact between two elastic rods

The current numerical example constitutes an initial assessment of the capability of CUF in modelling dynamic contact and impact. Two elastic rods are considered, as shown in Figure 8, and one rod impacts the other under a prescribed initial velocity v_0 = -0.1 [unit/s]. Both rods have the following material characteristics: Young's modulus E = 100.0, and Poisson's ratio ν = 0.30. The CUF analysis is performed in an explicit dynamics solver based on the central difference scheme, using CUF theories for the structural modelling. Reference numerical solutions have been developed using ABAQUS -3D/Explicit. A time period T = [0, 1.0] has been considered for the analysis, with a time step Δt = 5.0e-4. Numerical damping has not been considered in the current analysis. The axial displacement u_y at the centre of the contact zone, as a function of time, has been plotted in Figure 9. The results of the initial assessment demonstrate the capability of CUF in modelling problems involving dynamic contact and impact.

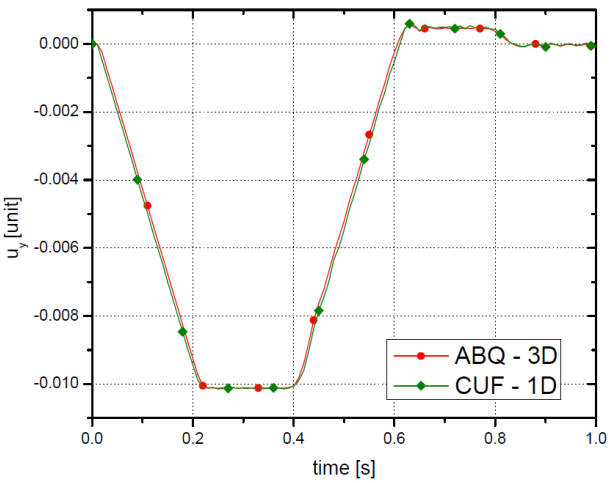

Figure 9: Axial displacement at the centre of the contact zone

4 CONCLUSION

The focus of the current work is on the development of contact modelling within the CUF framework. Node-to-node contact discretisation with the penalty approach to contact enforcement was considered, and the resulting nonlinear problem was implicitly solved using the Newton-Raphson method. The structural modelling was done using 1D CUF models with Lagrange polynomials being used to enrich the cross-sectional kinematics, resulting in a high-fidelity layer-wise model. Numerical assessments were performed to demonstrate the contact capabilities in CUF, and the results suggest that

1. The CUF solutions are in very good agreement with reference 3D-FEA, thus verifying the capability of the current framework in modelling contact.
2. The CUF-LW approach leads to accurate interlaminar stress fields, as well as transverse stretching, with about an order of magnitude reduction in the computational size and over a 4-fold improvement in the computational time, when compared to 3D-FEA.
3. Initial assessments on dynamic contact and impact demonstrate the capability of the CUF theories in accurately modelling such phenomena.

Future works include the further development of the explicit framework based on CUF, and its application to impact analysis of composite structures.

5 ACKNOWLEDGEMENTS

This research work has been carried out within the project ICONIC (Improving the Crashworthiness of Composite Transportation Structures), funded by the European Union Horizon 2020 Research and Innovation program under the Marie Skłodowska-Curie Grant agreement No. 721256, and the project FULLCOMP (Fully Integrated Analysis, Design, Manufacturing, and Health-Monitoring of Composite Structures), funded by the European Union Horizon 2020 Research and Innovation program under the Marie Skłodowska-Curie Grant agreement No. 642121.

REFERENCES

[1] M. A. Puso and T. A. Laursen. A mortar segment-to-segment contact method for large deformation solid mechanics. *Computer methods in applied mechanics and engineering*, *193*(6-8), pp.601-629 (2004).

[2] H. Hertz. Uber die beruhrung fester elastischer korper (on the contact of elastic solids). *J. fur die Reine Angew. Math.*, 92, pp.156-171 (1881).

[3] P. Wriggers. *Computational Contact Mechanics*. Springer-Verlag (2006).

[4] A. Francavilla and O. C. Zienkiewicz. A note on numerical computation of elastic contact problems. *International Journal for Numerical Methods in Engineering*, *9*(4), pp.913-924 (1975).

[5] J. O. Hallquist, G. L. Goudreau and D. J. Benson. Sliding interfaces with contact-impact in large-scale Lagrangian computations. *Computer methods in applied mechanics and engineering*, *51*(1-3), pp.107-137 (1985).

[6] J. C. Simo, P. Wriggers and R. L. Taylor. A perturbed Lagrangian formulation for the finite element solution of contact problems. *Computer methods in applied mechanics and engineering*, *50*(2), pp.163-180 (1985).

[7] P. Papadopoulos and R. L. Taylor. A mixed formulation for the finite element solution of contact problems. *Computer Methods in Applied Mechanics and Engineering*, *94*(3), pp.373-389 (1992).

[8] G. Zavarise and L. De Lorenzis. The node-to-segment algorithm for 2D frictionless contact: classical formulation and special cases. *Computer Methods in Applied Mechanics and Engineering*, *198*(41-44), pp.3428-3451 (2009).

[9] F. B. Belgacem, P. Hild and P. Laborde. Approximation of the unilateral contact problem by the mortar finite element method. *Comptes Rendus de l'Academie des Sciences Series I Mathematics*, *324*(1), pp.123-127 (1997).

[10] G. Zavarise and P. Wriggers. A segment-to-segment contact strategy. *Mathematical and Computer Modelling*, *28*(4-8), pp.497-515 (1998).

[11] T. W. McDevitt and T. A. Laursen. A mortar-finite element formulation for frictional contact problems. *International Journal for Numerical Methods in Engineering*, *48*(10), pp.1525-1547 (2000).

[12] M. A. Puso and T. A. Laursen. A mortar segment-to-segment frictional contact method for large deformations. *Computer methods in applied mechanics and engineering*, *193*(45-47), pp.4891-4913 (2004).

[13] E. Carrera, M. Cinefra, M. Petrolo and E. Zappino. *Finite element analysis of structures through unified formulation*. John Wiley & Sons (2014).

[14] A. G. de Miguel, I. Kaleel, M. H. Nagaraj, A. Pagani, M. Petrolo and E. Carrera. Accurate evaluation of failure indices of composite layered structures via various FE models. *Composites Science and Technology*, *167*, pp.174-189 (2018).

[15] E. Carrera and M. Petrolo. Refined beam elements with only displacement variables and plate/shell capabilities. *Meccanica*, *47*(3), pp.537-556 (2012).